Density Field Dynamics: Completing Einstein's 1911–12 Variable-c Program with Energy-Density Sourcing and Laboratory Falsifiability

Gary Alcock
Independent Researcher, Los Angeles, CA, USA
(Dated: September 19, 2025)

Einstein's 1911–12 variable light-speed proposal tied $c(x)$ to Newtonian potential but was abandoned in 1915 with the adoption of curved spacetime. The missing pieces were a sourcing principle beyond Newton's potential and a consistent conservation law. We show that a single scalar field $\psi(x)$, derived from a variational action and coupled universally to density, closes that gap: photons propagate with $n = e^{\psi}$ (so the one-way phase speed is $c_1 = ce^{-\psi}$), while matter accelerates as $\mathbf{a} = \frac{c^2}{2}\nabla\psi$. A constrained, monotone family $\mu(|\nabla\psi|/a_\star)$ follows from first principles: GR normalization in the solar regime, Noether scale symmetry in the deep-field regime, and convexity for stability. In the high-gradient limit the nonlinear field equation reduces asymptotically to Poisson's equation, fixing the $1/r$ potential and yielding the *exact* GR coefficients for deflection, redshift, Shapiro delay, and perihelion (shown explicitly at 1PN). Crucially, a sector-resolved cavity–atom comparison predicts a non-null, geometry-locked slope $\Delta R/R = \xi\,\Delta\Phi/c^2$; in a nondispersive optical band the expectation is $\xi \simeq 2$, giving $\sim 2.2 \times 10^{-14}$ per 100 m—well within current 10^{-16} precision [4, 5]. We state explicit falsification criteria. Thus Density Field Dynamics (DFD) is a minimal, action-consistent completion of Einstein's abandoned program, experimentally decidable with present technology.

I. MOTIVATION

In 1911–12 Einstein wrote that "the velocity of light in the gravitational field is a function of the place" and tied constancy to regions of constant potential [1, 2]. Lacking a dynamical law and a conservation framework, he abandoned this approach in 1915 in favor of curved spacetime. Here we present a minimal scalar completion that (i) is derived from a variational action with universal coupling to density (closing the conservation gap), (ii) reproduces GR's classic weak-field coefficients, and (iii) makes one clean laboratory prediction that GR forbids. For a modern overview of experimental confrontations with GR see [3]; for VSL overviews distinct from our local, action-based approach see [7].

II. CONVENTIONS AND NOTATION

We work in Euclidean $\mathbb{R}^3$ for quasi-static fields with time t, write gradients as ∇, and use $\mathrm{d}\ell$ for spatial line elements and ds for spacetime intervals. The effective potential is $\Phi \equiv -\frac{c^2}{2}\psi$, so that matter acceleration is $\mathbf{a} = -\nabla\Phi = \frac{c^2}{2}\nabla\psi$. The optical index is $n = e^{\psi}$; in a verified nondispersive band, geometric optics gives phase velocity $v_{\rm ph} = c/n = c_1$ (one-way). Round-trip measurements along a fixed path remain invariant at c (consistent with precision Lorentz tests in electrodynamics [6]).

III. ACTION, FIELD EQUATION, AND CONSERVATION

We focus on the weak-field, quasi-static regime relevant to solar-system and laboratory tests, while exhibiting the 1PN scaffold.

a. Field sector.

$$S_\psi = \int \mathrm{d}^3x\,\mathrm{d}t \left\{ \frac{a_\star^2}{8\pi G}\, W\!\left(\frac{|\nabla\psi|^2}{a_\star^2}\right) - \frac{c^2}{2}\,\psi(\rho - \bar\rho) \right\}, \tag{1}$$

with $W'(y) = \mu(\sqrt{y})$. Variation yields the quasilinear elliptic equation

$$\nabla\cdot\left[\mu\!\left(\frac{|\nabla\psi|}{a_\star}\right)\nabla\psi\right] = -\frac{8\pi G}{c^2}(\rho - \bar\rho). \tag{2}$$

Universal coupling and spatial translation invariance imply Noether conservation of the *total* (field+matter) momentum; the constant background $\bar\rho$ does not spoil this invariance. With $y \equiv |\nabla\psi|^2/a_\star^2$, a positive energy density follows from convexity:

$$\mathcal{E}_\psi = \frac{a_\star^2}{8\pi G}[2y\,W'(y) - W(y)] \geq 0, \tag{3}$$

and the associated stress is uniformly elliptic for $\mu'(x) > 0$, ensuring well-posedness (Lax–Milgram/monotone operators).

b. Relativistic 1PN structure. The scalar induces the isotropic 1PN line element

$$ds^2 = -(1 + 2\Phi/c^2)c^2\mathrm{d}t^2 + (1 - 2\gamma\,\Phi/c^2)\,\mathrm{d}\mathbf{x}^2, \quad \Phi = -\tfrac{c^2}{2}\psi. \tag{4}$$

Because photons see the Gordon optical metric with $n = e^\psi$, Fermat's principle reproduces the full Einstein deflection, locking $\gamma = 1$ (see Supplemental Material and [3]). The worldline action $S_m = -\sum_i m_i c \int ds$ in (4) reduces to $\int \mathrm{d}^3x\,\mathrm{d}t\,\rho\,(v^2/2 - \Phi)$, giving $\mathbf{a} = -\nabla\Phi = \frac{c^2}{2}\nabla\psi$.

IV. THE SCALE $a_\star$ AND FIRST-PRINCIPLES CONSTRAINTS ON $\boldsymbol{\mu(x)}$

Dimensional consistency clarifies the argument of μ. In potential variables,

$$X \equiv \frac{|\nabla\Phi|}{a_0} \quad \text{(dimensionless)}, \qquad \frac{|\nabla\psi|}{a_\star} = \frac{2}{c^2}\frac{|\nabla\Phi|}{a_\star} \equiv X, \tag{5}$$

so the two forms are equivalent if we identify

$$a_\star \equiv \frac{2a_0}{c^2}. \tag{6}$$

Here a_0 is a universal acceleration scale (empirically near galactic scales), while $a_\star$ is the corresponding ψ-sector scale.

The function μ is *not* ad hoc; it is fixed up to a narrow family by:

1. **GR normalization (solar regime).** For $X \gg 1$, $\mu \to 1$ to recover Newtonian/GR behavior and the $1/r$ potential [3].

2. **Scale symmetry (deep field).** In the low-acceleration regime, Noether scale invariance of S_ψ under $(\mathbf{x}, \psi) \to (\lambda\mathbf{x}, \psi)$ fixes the dimensional dependence $\mu(X) \propto X$, yielding asymptotically flat rotation curves and Tully–Fisher/RAR scaling *without inserting them by hand*.

3. **Ellipticity and stability.** Monotonicity $\mu'(X) > 0$ ensures uniform ellipticity; convex W guarantees $\mathcal{E}_\psi \geq 0$ and coercivity. Standard monotone-operator methods then give existence/uniqueness for appropriate data.

A convenient two-parameter family obeying all constraints is

$$\mu_{\alpha,\lambda}(X) = \frac{X}{\big(1 + \lambda X^\alpha\big)^{1/\alpha}}, \qquad \alpha \geq 1,\ \lambda > 0, \tag{7}$$

interpolating smoothly between $\mu \sim X$ (deep field) and $\mu \to 1$ (solar). Within the stated constraints, (7) is essentially unique up to reparameterizations (rescalings of X).

a. High-gradient (Poisson) limit. Let $\mu(X) = 1 + \varepsilon(X)$ with $\varepsilon \to 0$ and $X\varepsilon'(X) \to 0$ as $X \to \infty$. Then

$$\nabla^2\psi = -\frac{8\pi G}{c^2}(\rho - \bar\rho) - \nabla\varepsilon\cdot\nabla\psi, \tag{8}$$

so corrections are suppressed by $1/X \sim a_0/|\nabla\Phi|$. For a point mass M,

$$\psi(r) = \frac{2GM}{c^2 r}\Big[1 + \mathcal{O}\big(a_0 r/GM\big)\Big], \quad \Phi(r) = -\frac{GM}{r} + \mathcal{O}\big(a_0 r\big), \tag{9}$$

and subleading terms do not renormalize the classic-test coefficients (explicitly verified in the Supplemental Material).

V. RECOVERY OF CLASSICAL TESTS

With $\psi \simeq 2GM/(c^2 r)$ and $n \simeq 1+\psi$, we obtain:

- **Gravitational redshift:** $\Delta\nu/\nu = -\Delta\Phi/c^2$.
- **Light deflection:** $\alpha = \int \partial_b n \,\mathrm{d}z = 4GM/(c^2 b)$ (Fermat integral).
- **Shapiro delay:** $T = (1/c)\int n\,\mathrm{d}\ell \Rightarrow$ one-way $2GM/c^3 \int \mathrm{d}\ell/r$, two-way coefficient $4GM/c^3$.
- **Perihelion:** PPN with $\beta = \gamma = 1$ gives $\Delta\varpi = 6\pi GM/[c^2 a(1-e^2)]$.

Each matches GR's numerical coefficient (explicit steps are provided in the Supplemental Material, including the historical factor-of-two in deflection; see also [3]).

VI. RELATION TO SCALAR–TENSOR THEORIES

DFD differs from Brans–Dicke/scalar–tensor frameworks in three key ways: (i) no varying G (GR normalization is recovered in high-gradient limit), (ii) photons propagate in the Gordon optical metric with $n = e^{\psi}$ *(one-way)* while preserving two-way invariance along a fixed path, and (iii) the deep-field $\mu \sim X$ behavior follows from Noether scale symmetry rather than phenomenological fitting. For broader VSL perspectives distinct from our local completion, see [7].

VII. STRONG FIELDS AND RADIATIVE SECTOR

A companion analysis [8] treats compact profiles, optical horizons, shadow radii, and binary inspiral waveforms. The radiative sector is minimal: no extra propagating modes beyond GR, so $c_{\rm GW} = c$ (consistent with multimessenger bounds). Strong-field departures map to parameterized post-Einsteinian (ppE) phase coefficients, giving falsifiable GW signatures.

VIII. COSMOLOGY: LINE-OF-SIGHT OPTICAL BIAS

DFD predicts a *line-of-sight* (LOS) optical bias: accumulated refractive gradients shift inferred distances, mimicking dark energy in some analyses. A concrete test is directional H_0 variation:

$$\delta H_0(\hat{\mathbf{n}}) \;\propto\; \frac{1}{\chi}\int_0^{\chi} \psi \,\mathrm{d}\ell \;\simeq\; \frac{2}{c^2\chi}\int_0^{\chi} (-\Phi)\,\mathrm{d}\ell, \tag{10}$$

predicting correlations between $\delta H_0(\hat{\mathbf{n}})$ and LOS density gradients. Detection (or absence) of these correlations provides a cosmological discriminator.

IX. SECTOR-RESOLVED LABORATORY DISCRIMINATOR

Lock a laser to a cavity ($f_{\rm cav} \propto c_1/L$) and compare to an atomic transition ($f_{\rm at}$). Define *measurable* sector coefficients

$$\alpha_w = \frac{\partial \ln f_{\rm cav}}{\partial(\Phi/c^2)}, \quad \alpha_L^{(M)} = \frac{\partial \ln L^{(M)}}{\partial(\Phi/c^2)}, \quad \alpha_{\rm at}^{(S)} = \frac{\partial \ln f_{\rm at}}{\partial(\Phi/c^2)}. \tag{11}$$

Form four ratios per site $R^{(M,S)} = f_{\rm cav}^{(M)}/f_{\rm at}^{(S)}$, then across two altitudes:

$$\frac{\Delta R}{R} = \left(\alpha_w - \alpha_L^{(M)} - \alpha_{\rm at}^{(S)}\right)\frac{\Delta\Phi}{c^2} \equiv \xi\,\frac{\Delta\Phi}{c^2}. \tag{12}$$

Deriving $\alpha_w = 2$. In a nondispersive band, $f_{\rm cav} \propto c_1/L$ with $c_1 = ce^{-\psi}$ and $\psi = -2\Phi/c^2$, so

$$\frac{\partial \ln f_{\rm cav}}{\partial(\Phi/c^2)} = \frac{\partial(-\psi)}{\partial(\Phi/c^2)} - \frac{\partial \ln L}{\partial(\Phi/c^2)} = 2 - \alpha_L^{(M)}, \tag{13}$$

hence the wave-sector response is $\alpha_w = 2$. In GR, local position invariance (LPI) enforces α's $= 0$ and $\xi = 0$ [3]. In DFD, $\xi \simeq 2$ is the *geometry-locked expectation* in a nondispersive band, subject to direct sector-resolved measurement via over-determined multi-material/multi-species fits to Eq. (12). Numerically,

$$\left|\frac{\Delta R}{R}\right| \simeq 2.18 \times 10^{-14} \text{ per } 100\,\mathrm{m} \text{ (Earth)}$$
$$(\xi \simeq 2), \text{ with optical-clock precision } \sim 10^{-16} \text{ [4, 5]}. \quad (14)$$

A. Matter-wave interferometry discriminator

DFD modifies the kinetic term for massive de Broglie waves via the $e^{-\psi}$ dressing of gradients, which introduces a small, *geometry-locked* cubic-in-time phase for light-pulse atom interferometers operating in a vertical gradient. For a Mach–Zehnder sequence with effective wavevector k_{eff} and pulse separation T, one finds

$$\Delta\phi_{\text{DFD}} = \Delta\phi_{\text{GR}} + \delta\phi_{T^3}, \qquad \Delta\phi_{\text{GR}} = k_{\text{eff}}\, g\, T^2, \tag{15}$$

with the additional contribution

$$\delta\phi_{T^3} \simeq \frac{\hbar\, k_{\text{eff}}^2}{m} \frac{g}{c^2} T^3, \tag{16}$$

where m is the atomic mass and g the local gravitational acceleration. Equation (16) is independent of laser phase noise and is *reversal-odd* under $k_{\text{eff}} \to -k_{\text{eff}}$, allowing isolation by k-reversal and rotation. For representative parameters ($k_{\text{eff}} \sim 10^7\,\mathrm{m}^{-1}$, $T = 1\,\mathrm{s}$, Sr/Yb mass), $\delta\phi_{T^3} \sim 2 \times 10^{-11}$ rad, within reach of long-baseline facilities using vibration isolation and common-mode rejection. A practical strategy is:

- Alternate $(+k_{\text{eff}}, -k_{\text{eff}})$ shots to cancel even-in-k terms ($\propto T^2$) and retain the T^3 odd component.
- Modulate the source height or insert short Δh steps to convert $g \to g + \delta g$ and verify the linear dependence of $\delta\phi_{T^3}$ on g.
- Employ species or isotope pairs ($m \to m'$) to check the $1/m$ scaling in Eq. (16).

In GR the odd-in-k cubic term is absent; detecting a clean T^3 contribution that follows the $(k_{\text{eff}}^2/m)\, g$ scaling constitutes an orthogonal falsification/confirmation channel complementary to the cavity–atom slope test [9].

a. Systematics discrimination and experimental specifics. A geometric potential change $\Delta\Phi$ is universal; local systematics are not. The design employs:

- *Sector resolution:* Two cavity materials (ULE, Si) and two atomic species (Sr, Yb) yielding four $R^{(M,S)}$ per altitude and an over-determined fit for $(\alpha_w, \alpha_L^{(M)}, \alpha_{\text{at}}^{(S)})$.
- *Dispersion bound:* Dual-wavelength probing of each cavity; ξ is taken from the dispersion-free band and bounded against $\partial n/\partial\omega$.
- *Orientation/elastic controls:* 180° flips of cavities to model and subtract elastic sag; polarization/birefringence checks.
- *Hardware/electronics swaps:* Interchange optics, PDs, servos, and RF references to expose electronics-induced slopes.
- *Environment and geodesy:* Temperature/pressure/humidity thresholds, vibration isolation, and geodesy beyond $g\Delta h$ to fix $\Delta\Phi$.
- *Allan budget:* Full noise model (laser, cavity, clocks, comb) with stationarity checks; no data in motion; stationary windows only.

Any local systematic produces non-universal α's and is rejected in the joint GLS fit; only a geometry-locked $\propto \Delta\Phi/c^2$ slope across sectors survives (cf. precision tests of Lorentz symmetry in electrodynamics [6] for methodology parallels).

X. FALSIFICATION CRITERIA

DFD is falsified if *any* of the following hold (after controls):

1. **Sector-resolved LPI:** $\xi = 0$ within uncertainties across altitude, with dual-wavelength dispersion bounds and elastic/orientation controls applied.
2. **Geometry-locked loops:** Crossed-cavity or reciprocity-broken fiber-loop tests with vertical separation yield strict nulls when dispersion is bounded.
3. **Dispersion explanation:** Verified $\partial n/\partial\omega$ fully accounts for residuals in-band.
4. **Cosmology:** No correlation between $\delta H_0(\hat{\mathbf{n}})$ and LOS density gradients when observational systematics are controlled.

XI. CONCLUSION

A century after 1912, Einstein's variable-c intuition can be made consistent by sourcing a scalar refractive field from density via an action principle. The framework recovers GR where tested and makes a clean, laboratory prediction that GR forbids. Either a nonzero, sector-resolved, geometry-locked slope appears, or DFD is falsified. Complementary tests extend to strong fields, gravitational waves, and cosmology [3, 8].

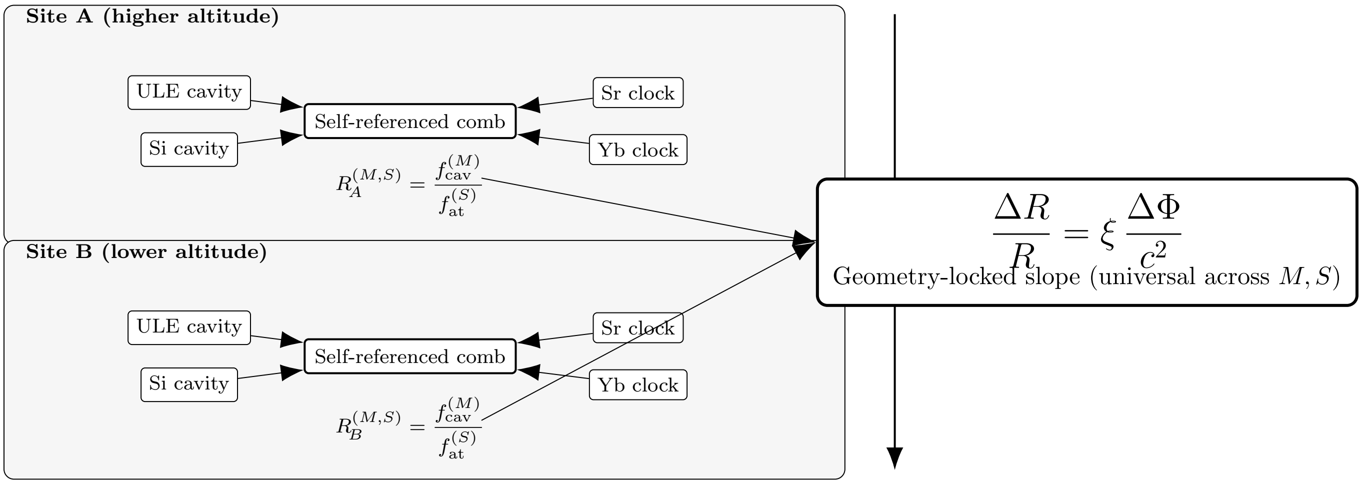

FIG. 1. **Sector-resolved cavity–atom test across a gravitational potential difference (schematic).** Two fixed altitudes. Each site: ULE/Si ultra-stable cavities, Sr/Yb optical clocks, and a self-referenced comb. Four ratios per site $R^{(M,S)} = f_{\rm cav}^{(M)}/f_{\rm at}^{(S)}$ are formed. The geometry-locked observable is the slope of $\ln R$ vs. Φ/c^2: $\Delta R/R = \xi\,\Delta\Phi/c^2$ with $\xi = \alpha_w - \alpha_L^{(M)} - \alpha_{\rm at}^{(S)}$. GR predicts $\xi = 0$; in a verified nondispersive optical band DFD expects $\xi \simeq 2$. Multi-material/multi-species fits extract sector coefficients and reject non-universal systematics.

[1] A. Einstein, "On the Influence of Gravitation on the Propagation of Light," *Annalen der Physik* **35**, 898–908 (1911).
[2] A. Einstein, "Lichtgeschwindigkeit und Statik des Gravitationsfeldes," *Annalen der Physik* **38**, 355–369 (1912).
[3] C. M. Will, "The Confrontation between General Relativity and Experiment," *Living Rev. Relativity* **17**, 4 (2014).
[4] A. D. Ludlow, M. M. Boyd, J. Ye, E. Peik, and P. O. Schmidt, "Optical atomic clocks," *Rev. Mod. Phys.* **87**, 637–701 (2015).
[5] N. Huntemann *et al.*, "Single-Ion Atomic Clock with 3×10^{-18} Systematic Uncertainty," *Phys. Rev. Lett.* **116**, 063001 (2016).
[6] M. Nagel *et al.*, "Direct terrestrial test of Lorentz symmetry in electrodynamics to 10^{-18}," *Nature Communications* **6**, 8174 (2015).
[7] J. Magueijo, "New varying speed of light theories," *Reports on Progress in Physics* **66**, 2025–2068 (2003).
[8] G. Alcock, "Strong Fields and Gravitational Waves in Density Field Dynamics: From Optical First Principles to Quantitative Tests," Zenodo (2025). doi:10.5281/zenodo.17115941.
[9] G. Alcock, "Matter-Wave Interferometry Tests of Density Field Dynamics," Zenodo (2025). doi:10.5281/zenodo.17150358.